

# An Intriguing X-ray Arc Surrounding the X-ray Source RX J053335–6854.9 toward the Large Magellanic Cloud

Justin D. Lowry<sup>1</sup>, You-Hua Chu<sup>1</sup>, Martín A. Guerrero<sup>1,2,3</sup>, Robert A. Gruendl<sup>1</sup>, Steven L. Snowden<sup>4</sup>, R. Chris Smith<sup>5</sup>

## ABSTRACT

*ROSAT* observations of the Large Magellanic Cloud (LMC) have revealed a large diffuse X-ray arc around the point source RX J053335–6854.9. The relative locations of the diffuse and point sources suggest that they might originate from a common supernova explosion. We have analyzed the physical properties of the diffuse X-ray emission and determined that it is most likely a supernova remnant in a low-density medium in the LMC. We have also analyzed the X-ray and optical observations of RX J053335–6854.9 and concluded that it is a foreground dMe star in the solar neighborhood. Therefore, despite their positional coincidence, these two X-ray sources are physically unrelated.

*Subject headings:* galaxies: ISM — Magellanic Clouds — supernova remnants — X-rays: ISM — X-rays: stars

## 1. Introduction

The *Röntgen X-ray Satellite (ROSAT)* observations of the Large Magellanic Cloud (LMC) have revealed a wealth of diffuse and compact X-ray sources (Snowden & Petre

---

<sup>1</sup>Astronomy Department, University of Illinois, 1002 W. Green Street, Urbana, IL 61801; jd-lowry@astro.uiuc.edu, chu@astro.uiuc.edu, mar@astro.uiuc.edu, gruendl@astro.uiuc.edu

<sup>2</sup>Visiting Astronomer, Cerro Tololo Inter-American Observatory, National Optical Astronomy Observatory, which is operated by the Association of Universities for Research in Astronomy, Inc. under cooperative agreement with the National Science Foundation.

<sup>3</sup>Now at Instituto Astrofísica de Andalucía (CSIC), Spain.

<sup>4</sup>Laboratory for High Energy Astrophysics, Code 662, NASA Goddard Space Flight Center, Greenbelt, MD 20771; snowden@riva.gsfc.nasa.gov

<sup>5</sup>Cerro Tololo Inter-American Observatory, National Optical Astronomy Observatory, Casilla 603, La Serena, Chile; csmith@noao.edu

1994; Haberl & Pietsch 1999; Sasaki, Haberl, & Pietsch 2002). Many large diffuse X-ray sources have sizes greater than 100 pc. Some of these diffuse sources are associated with superbubbles and supergiant shells, and others seem to originate from fields unbounded by interstellar structures identifiable at optical or radio wavelengths (Dunne et al. 2001; Points et al. 2001).

Among the large diffuse X-ray sources, we have identified two objects whose diffuse X-ray emissions have ring morphologies and are centered on point sources. These two objects are intriguing because they are not bounded by superbubbles and the relative locations of the point source and the diffuse X-ray emission appear to suggest a physical association. The first object, at  $5^{\text{h}}07^{\text{m}}36^{\text{s}}$ ,  $-68^{\circ}47'52''$  (J2000), is projected in the vicinity of the superbubble N103 surrounding the star cluster NGC 1850. A detailed analysis of this object shows that the large X-ray ring, 150 pc in diameter, is most likely a supernova remnant (SNR) formed in the low-density halo of the LMC and the central point source might be an X-ray binary in the cluster HS122, but the relationship between the SNR and the X-ray binary is uncertain (Chu et al. 2000).

The second object, shown in Figure 1, is projected on the eastern rim of the supergiant shell LMC-3 (Goudis & Meaburn 1978). Its  $\sim 9.5$  angular diameter corresponds to  $\sim 140$  pc, if it is in the LMC at a distance of 50 kpc (Feast 1999). The *ROSAT* Position Sensitive Proportional Counter (PSPC) mosaic (Snowden & Petre 1994) in Figure 1b shows semi-circular diffuse X-ray emission centered on the point source RX J053335–6854.9 at  $5^{\text{h}}33^{\text{m}}36^{\text{s}}$ ,  $-68^{\circ}54'55''$  (J2000). The *ROSAT* High Resolution Imager (HRI) mosaic (Chu & Snowden 1998) in Figure 1c, having a much higher angular resolution, shows diffuse X-ray emission in an east-north-west arc centered on the point source. RX J053335–6854.9 is coincident with a 14th mag stellar object in the Digitized Sky Survey (DSS). To determine the origin of the diffuse X-ray emission, we have analyzed the *ROSAT* observations in conjunction with optical images and high-dispersion, long-slit spectra of the underlying  $10^4$  K ionized interstellar gas. To determine the nature of the point source, we have examined both the photometric and spectral properties of its optical counterpart, and compared them with the spectral properties of the X-ray source. The results of our analysis are reported in this paper.

## 2. Observations

### 2.1. *ROSAT* X-ray Observations

*ROSAT* observations of RX J053335–6854.9 and its surrounding diffuse X-ray emission have been made with both the PSPC and the HRI detectors. The PSPC is sensitive in the

energy range 0.1–2.4 keV and has a 45% spectral resolution with on-axis angular resolution of  $\sim 25''$  at 1 keV. The HRI is sensitive at 0.1–2.0 keV; it has a negligible spectral resolution, but a high on-axis angular resolution of  $5''$ .

We have retrieved all *ROSAT* observations where RX J053335–6854.9 falls within  $45'$  and  $20'$  from the field center for the PSPC and HRI, respectively. These observations are listed with their exposure times, locations, original targets of the observations, and the offset of RX J053335–6854.9 from the field center in Table 1. Note that for all PSPC observations, RX J053335–6854.9 lies either close to or outside the circular window support structure of  $40'$  diameter. For the former, the wobbling of the telescope moves the source in and out of the shadow of the window support ring and decreases the number of counts, while for the latter the detector sensitivity is reduced and the point spread function is degraded at large off-axis angles. Therefore, we used the PSPC observations to carry out only the spectral analysis and used the higher resolution HRI observations for morphological analysis and comparisons with optical images.

We have used the PROS<sup>6</sup> software package within IRAF<sup>7</sup> for spatial and spectral analyses of these observations. To improve the S/N, we merged the PSPC observations centered on SN 1987A with exposure times  $\geq 9$  ks (see Table 1) to produce a 90 ks equivalent exposure, and extracted spectra from the combined data for further analysis. The other PSPC data were deemed to be less useful and were not used.

## 2.2. Optical Images

Optical images were taken at the Cerro Tololo Inter-American Observatory (CTIO) with a CCD camera on the Curtis Schmidt telescope. The observations were part of the Magellanic Cloud Emission-Line Survey (MCELS) by Smith et al. (1999). The detector was the SITe2048 #5 CCD. Its  $24 \mu\text{m}$  pixel size corresponds to  $2''.3$ . Images were obtained with the following filters and exposure times:  $\text{H}\alpha$  ( $\lambda_c = 6568 \text{ \AA}$ , FWHM =  $28 \text{ \AA}$ ), 150 s;  $[\text{O III}]$  ( $\lambda_c = 5023 \text{ \AA}$ , FWHM =  $40 \text{ \AA}$ ), 600 s;  $[\text{S II}]$  ( $\lambda_c = 6738 \text{ \AA}$ , FWHM =  $50 \text{ \AA}$ ), 600 s; green continuum ( $\lambda_c = 5130 \text{ \AA}$ , FWHM =  $155 \text{ \AA}$ ), 300 s; red continuum ( $\lambda_c = 6852 \text{ \AA}$ , FWHM =  $95 \text{ \AA}$ ), 300 s. The  $\text{H}\alpha$ ,  $[\text{S II}]$ , and red continuum images were obtained on 1998 November 27, and the  $[\text{O III}]$  and green continuum images were obtained on 2000 December 30. The

---

<sup>6</sup>PROS/XRAY Data Analysis System, <http://hea-www.harvard.edu/PROS/pros.shtml>

<sup>7</sup>Image Analysis and Reduction Facility, IRAF is distributed by the National Optical Astronomy Observatories operated by the Association of Universities for Research in Astronomy, Inc., under cooperative agreement with the National Science Foundation.

emission-line images of RX J053335–6854.9 and its vicinity are presented in Figure 2.

### 2.3. High-Dispersion Spectra

To determine the radial velocity of the optical counterpart of RX J053335–6854.9 and to examine the kinematics of the  $10^4$  K ionized gas underlying the diffuse X-ray emission, we obtained high-dispersion spectroscopic observations using the echelle spectrograph on the Blanco 4 m telescope at CTIO on 2002 June 24. The spectrograph was used with the 79 line  $\text{mm}^{-1}$  echelle grating and the long-focus red camera in the single-order, long-slit mode. This observing configuration provided a reciprocal dispersion of  $3.4 \text{ \AA mm}^{-1}$  and covered the  $\text{H}\alpha$  and  $[\text{N II}] \lambda\lambda 6548, 6584$  lines over a slit length of  $\sim 3'$ . The SITE2048 #6 CCD used has a pixel size of  $24 \mu\text{m}$ , which corresponds to  $\sim 3.7 \text{ km s}^{-1} \text{ pixel}^{-1}$  along the dispersion direction and  $0''.26 \text{ pixel}^{-1}$  along the slit. The slit width was  $1''.8$  and the resultant instrumental FWHM was  $15 \text{ km s}^{-1}$ . The angular resolution, determined by the seeing, was  $2''$ . The slit was oriented at  $\text{PA} = 345^\circ$  and the total integration time was 900 s.

## 3. Discussion: Physical Nature of the X-ray Sources

The X-ray point source RX J053335–6854.9 is projected within the LMC and apparently surrounded by the diffuse X-ray arc. Below we discuss the nature of the diffuse emission and the point source individually.

### 3.1. Physical Nature of the X-ray Arc

The circular boundary of the diffuse X-ray emission surrounding RX J053335–6854.9 suggests that the hot gas may have been energized by a supernova explosion at its geometric center. The angular radius varies from  $4'$  on the east side to  $5'.5$  on the west side. This diffuse X-ray emission region does not show morphological correspondence with optical emission. As shown in Figure 2, long ( $> 20'$ ) optical filaments exist but are associated with the supergiant shell LMC-3 and do not delineate the X-ray emission region. From the morphology alone, the hot gas responsible for the diffuse X-ray emission does not appear to be associated with the cooler gas responsible for the optical emission.

It is unlikely that this diffuse X-ray source is associated with a SNR in the Galactic plane (within 500 pc), because its linear size ( $< 2 \text{ pc}$ ) implies a very young age and it would have been much brighter. The probability is also small for this source to originate from a SNR in

the Galactic halo, because massive stars do not reside in the halo and the low stellar density in the halo implies a very low Type Ia supernova rate. On the other hand, its projected location in the LMC is within a large-scale star-forming region where the supernova rate is expected to be high; therefore, it is most likely that a SNR in the LMC is responsible for this diffuse X-ray emission. The linear radius of the X-ray emission region, 60–82 pc, is larger than those of most SNRs, a few tens of pc in diameter, but is reasonable for SNRs formed in a low-density medium.

The physical conditions of the X-ray-emitting gas can be derived from the observed X-ray spectra, which are a convolution of the intrinsic spectra, the intervening interstellar absorption, and the PSPC response function. The contribution of the absorption and response function to the spectra is energy-dependent, therefore it is necessary to model the spectra in order to determine the temperature and emission measure of the X-ray sources. The diffuse emission appears to originate from hot ionized gas therefore we used the Raymond & Smith (1977) models of thin plasma emission and the Morrison & McCammon (1983) models of absorption to simulate the observed spectra, and determined the best fit by  $\chi^2$  minimization.

The best-fit model for the background-subtracted PSPC spectrum (see Figure 3a) gives a plasma temperature of  $kT \simeq 0.3$  keV, an absorption column density of  $N_{\text{H}} = 4 \times 10^{20} \text{ cm}^{-2}$ , and a normalization factor  $A = 10^{10.7} \text{ cm}^{-5}$ . This plasma temperature is within the range commonly seen in SNRs. The rms electron density can be determined from the normalization factor  $A = N_{\text{e}}^2 V / (4\pi D^2)$ , where  $N_{\text{e}}$  is the electron density of the plasma,  $V$  is the volume of the X-ray-emitting plasma, and  $D$  is the distance to the X-ray source. Assuming a filled hemispherical emitting volume with a 70 pc radius, the rms  $N_{\text{e}}$  is  $\sim 0.03 \text{ cm}^{-3}$ , which is lower by at least an order of magnitude than most SNRs in the LMC. If the volume filling factor  $f$  of the X-ray-emitting plasma is less than 1, the density would be  $f^{-1/2}$  times higher, but still lower than those of most SNRs. The total thermal energy of the hot gas is  $\sim 8 \times 10^{49}$  ergs. The unabsorbed X-ray flux for the diffuse emission is  $\sim 9 \times 10^{-13} \text{ ergs cm}^{-2} \text{ s}^{-1}$ , and the X-ray luminosity is  $\sim 3 \times 10^{35} \text{ ergs s}^{-1}$  in the 0.5–2.0 keV band. Both the thermal energy and X-ray luminosity are similar to those observed in mature Magellanic Cloud SNRs  $\sim 10^4$  yr of age (Williams et al. 1997, 1999).

The physical properties of the diffuse X-ray emission around RX J053335–6854.9 are fully consistent with those of a mature SNR in a low-density medium, much like the large X-ray ring around RX J050736–6847.8 (Chu et al. 2000). The low density of the ambient interstellar medium explains the large size and the absence of a detectable optical shell.

The association of the diffuse X-ray arc with a SNR is further supported by the high-velocity ionized gas detected in our echelle observation. The echellogram in Figure 4 shows

two nebular components. The first component has a fairly uniform surface brightness and a nearly constant velocity, at  $V_{\text{Hel}} = 279 \pm 4 \text{ km s}^{-1}$ , along the entire slit length. This component originates from a large-scale diffuse ionized medium in the LMC. The second component is blue-shifted from the stationary component, and the velocity offset varies from  $< 50 \text{ km s}^{-1}$  at  $0'.5$  south of RX J053335–6854.9 to  $\sim 100 \text{ km s}^{-1}$  at  $1'.8$  north of RX J053335–6854.9. The high-velocity features are fainter than the large-scale diffuse component so that only the brightest feature,  $\sim 20''$  south of the star, can be identified with a filament in the emission-line images (compare Figures 2 and 4). The spatial scale and magnitude of velocity offset of this nebular component are similar to those seen in SNRs in the LMC (Chu & Kennicutt 1988). It is possible that this high-velocity nebular component is associated with the SNR responsible for the diffuse X-ray arc. While the SNR is in a low-density medium in general, there may exist small dense clouds which are shocked and give rise to the high-velocity nebular emission. The scarcity of the dense clouds in a low-density medium prevents the formation of a dense SNR shell structure.

### 3.2. Physical Nature of the Point Source

The X-ray point source RX J053335–6854.9 appears to be coincident with a 14th mag star shown in the DSS. The position of RX J053335–6854.9 measured from the HRI image (RH600640N00) is  $5^{\text{h}}33^{\text{m}}36^{\text{s}}.0$ ,  $-68^{\circ}54'55''$  (J2000). The star has been cataloged in the Guide Star Catalog 2.2 as GSC2.2 S013200256362 at  $5^{\text{h}}33^{\text{m}}35^{\text{s}}.2$ ,  $-68^{\circ}54'54''$  (J2000), in the 2 Micron All Sky Survey (2MASS) as PSC 05333511–6854544 at an almost identical position, and in the US Naval Observatory-A2.0 catalog as USNO-A2.0 0150-03257930 at  $5^{\text{h}}33^{\text{m}}35^{\text{s}}.3$ ,  $-68^{\circ}54'54''$  (J2000). The apparent offset between the X-ray source and the optical star,  $4''.5$ , can be accounted for by the uncertainty in the aspect solution of the *ROSAT* pointing. Therefore, we consider the X-ray and optical sources coincident.

The photometric measurements of the star given by the catalogs are:  $B = 16.9$  and  $R = 14.4$  in USNO-A2.0;  $B = 16.56 \pm 0.53$  and  $R = 14.47 \pm 0.19$  in GSC 2.2; and  $J = 11.51 \pm 0.02$ ,  $H = 10.88 \pm 0.02$ , and  $K = 10.68 \pm 0.02$  in 2MASS. The colors of this star,  $B - R = 2.1 \pm 0.7$ ,  $R - K = 3.8 \pm 0.2$ , and  $J - K = 0.827 \pm 0.04$ , are consistent with a red star with a spectral type of M2–M3 (Cox 2000). As the distance to this star is unknown, it can be a supergiant in the LMC, a giant in the Galactic halo, or a dwarf in the solar neighborhood.

These three possibilities can be distinguished by the radial velocity ( $V_{\text{Hel}}$ ) of the star:  $\sim 300 \text{ km s}^{-1}$  in the LMC, moderate to high velocities in the Galactic halo, and low velocities in the solar neighborhood. We have extracted a sky-subtracted spectrum of this star from

our echelle observation and plotted it in Figure 4c. The most prominent spectral feature of the star in this wavelength range is the  $H\alpha$  emission line at  $V_{\text{Hel}} \sim 0 \text{ km s}^{-1}$ , or  $V_{\text{LSR}} \sim -14 \text{ km s}^{-1}$ . This small radial velocity strongly argues for this star to be located in the solar neighborhood. Thus we further conclude that the star is a dwarf M2–M3 star with  $H\alpha$  emission, one of those commonly called dMe stars. Adopting a dwarf luminosity class, the distance to the star is found to be 60–80 pc.

To determine whether RX J053335–6854.9 and the star are physically associated, we examine the X-ray spectral properties. The background-subtracted PSPC spectrum of RX J053335–6854.9 in Figure 3b displays a spectral shape typical for stellar coronal emission. As dMe stars are known to exhibit coronal activity, it is likely that RX J053335–6854.9 and this dMe star are physically associated. We have used the thin plasma emission model of Raymond & Smith (1977) to fit the PSPC spectrum. The best-fit model gives a plasma temperature of  $kT = 0.26 \text{ keV}$  and an absorption column density of  $N_{\text{H}} = 2 \times 10^{19} \text{ cm}^{-2}$ . The small absorption column density indicates a small distance. Adopting the distance of the dMe star, 60–80 pc, the X-ray luminosity of RX J053335–6854.9 is  $(2\text{--}3) \times 10^{28} \text{ ergs s}^{-1}$  in the 0.5–2.0 keV range. This X-ray luminosity is completely consistent with those expected from dMe stars (Rucinski 1984). We therefore conclude that the X-ray point source RX J053335–6854.9 is physically associated with the dMe star.

#### 4. Conclusions

*ROSAT* observations of the LMC have revealed a large diffuse X-ray arc in projection around the point source RX J053335–6854.9. The relative locations of the diffuse and point sources suggest that they might originate from a common supernova explosion. We have analyzed the physical properties of the diffuse X-ray emission and determined that it is most likely a SNR in a predominantly low-density medium. We have also analyzed the X-ray and optical observations of RX J053335–6854.9 and concluded that it is a dMe star in the solar neighborhood. Therefore, these two X-ray sources are physically unrelated. As dMe stars are the most prevalent stellar X-ray sources in the solar neighborhood (Schmitt, Fleming, & Giampapa 1995), and as the cooling time for a SNR in a low-density medium is long, the probability for the superposition of a nearby dMe star with a large SNR in the LMC is not negligible.

The project was partially supported by the NASA grant NAG 5-8104. The optical images from the Magellanic Cloud Emission-line Surveys were obtained with support from the Dean B. McLaughlin fund at the University of Michigan and NSF grant AST-9540747.

This research has made use of the SIMBAD database, operated at CDS, Strasbourg, France, and the Digital Sky Survey produced at the Space Telescope Science Institute under U.S. Government grant NAG W-2166. We have also used data products from the 2MASS, which is a joint project of the University of Massachusetts and the Infrared Processing and Analysis Center/California Institute of Technology, funded by NASA and NSF.

## REFERENCES

- Chu, Y.-H., & Kennicutt, R. C. 1988, *AJ*, 95, 1111
- Chu, Y.-H., Kim, S., Points, S. D., Petre, R., & Snowden, S. L. 2000, *AJ*, 119, 2242
- Chu, Y.-H., & Snowden, S. L. 1998, *AN*, 319, 101
- Cox, A. N. 2000, *Allen's Astrophysical Quantities*, (AIP Press)
- Dunne, B. C., Points, S. D., & Chu, Y.-H. 2001, *ApJS*, 119
- Feast, M. 1999, in *IAU Symp. 190, New Views of the Magellanic Clouds*, ed. Y.-H. Chu et al. (San Francisco: ASP), 542
- Goudis, C., & Meaburn, J. 1978, *A&A*, 68, 189
- Haberl, F., & Pietsch, W. 1999, *A&AS*, 139, 277
- Morrison, R., & McCammon, D. 1983, *ApJ*, 270, 119
- Points, S. D., Chu, Y.-H., & Smith, R. C. 2001, *ApJS*, 136
- Raymond, J. C., & Smith, B. W. 1977, *ApJS*, 35, 419
- Rucinski, S. M. 1984, *A&A*, 132, L9
- Sasaki, M., Haberl, F., & Pietsch, W. 2002, *A&A*, 392, 103
- Schmitt, J. M. M. M., Fleming, T. A., & Giampapa, M. S. 1995, *ApJ*, 450, 392
- Smith, R. C., et al. 1999, in *IAU Symp. 190, New Views of the Magellanic Clouds*, ed. Y.-H. Chu et al. (San Francisco: ASP), 28
- Snowden, S. L., & Petre, R. 1994, *ApJ*, 436, L123
- Williams, R. M., Chu, Y., Dickel, J. R., Beyer, R., Petre, R., Smith, R. C., & Milne, D. K. 1997, *ApJ*, 480, 618



Williams, R. M., Chu, Y., Dickel, J. R., Smith, R. C., Milne, D. K., & Winkler, P. F. 1999,  
ApJ, 514, 798

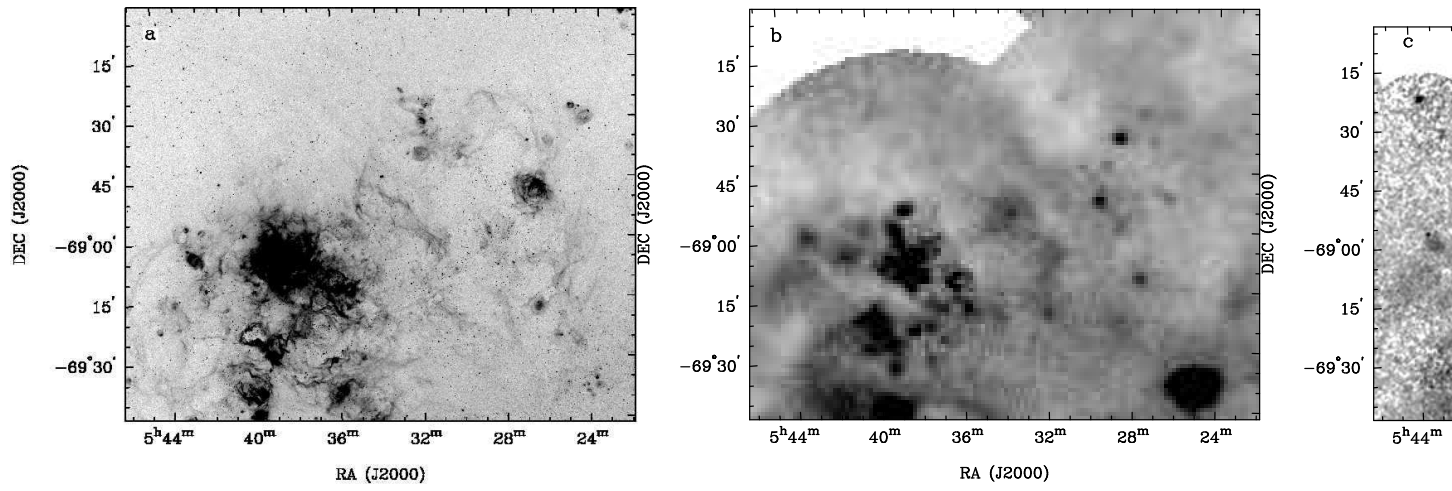


Fig. 1.— (a)  $H\alpha$  image of RX J053335–6854.9 and its vicinity. (b) *ROSAT* PSPC mosaic of the same field in the 0.1–2.4 keV band. (c) *ROSAT* HRI mosaic of the same field. RX J053335–6854.9 is located at the field center.

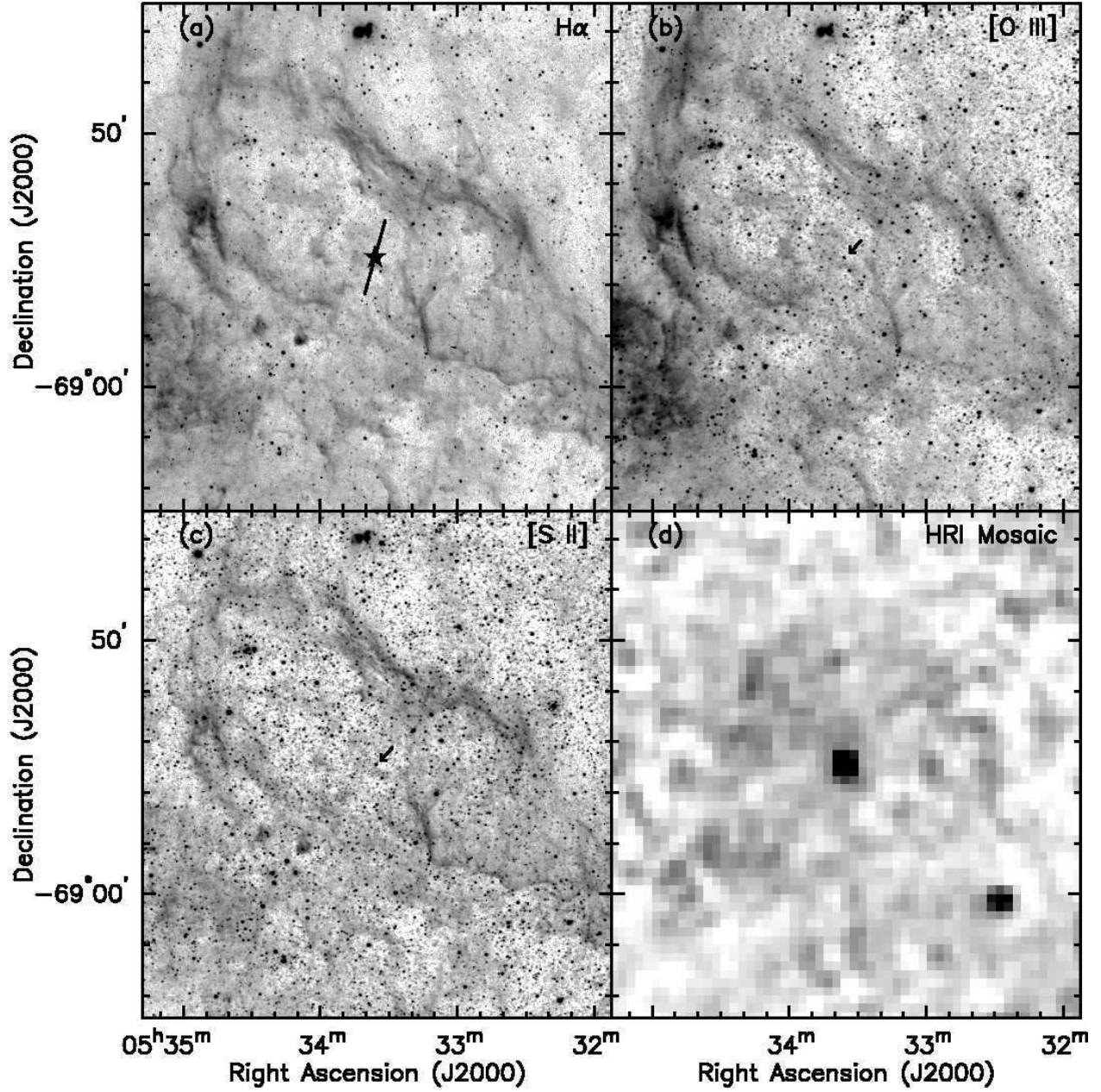


Fig. 2.— (a) H $\alpha$ , (b) [O III], (c) [S II], and (d) *ROSAT* HRI images of the region centered at RX J053335–6854.9. The stellar counterpart of RX J053335–6854.9 is marked by “ $\star$ ” in (a) and arrows in (b) and (c). The slit position of the echelle observation is marked in (a).

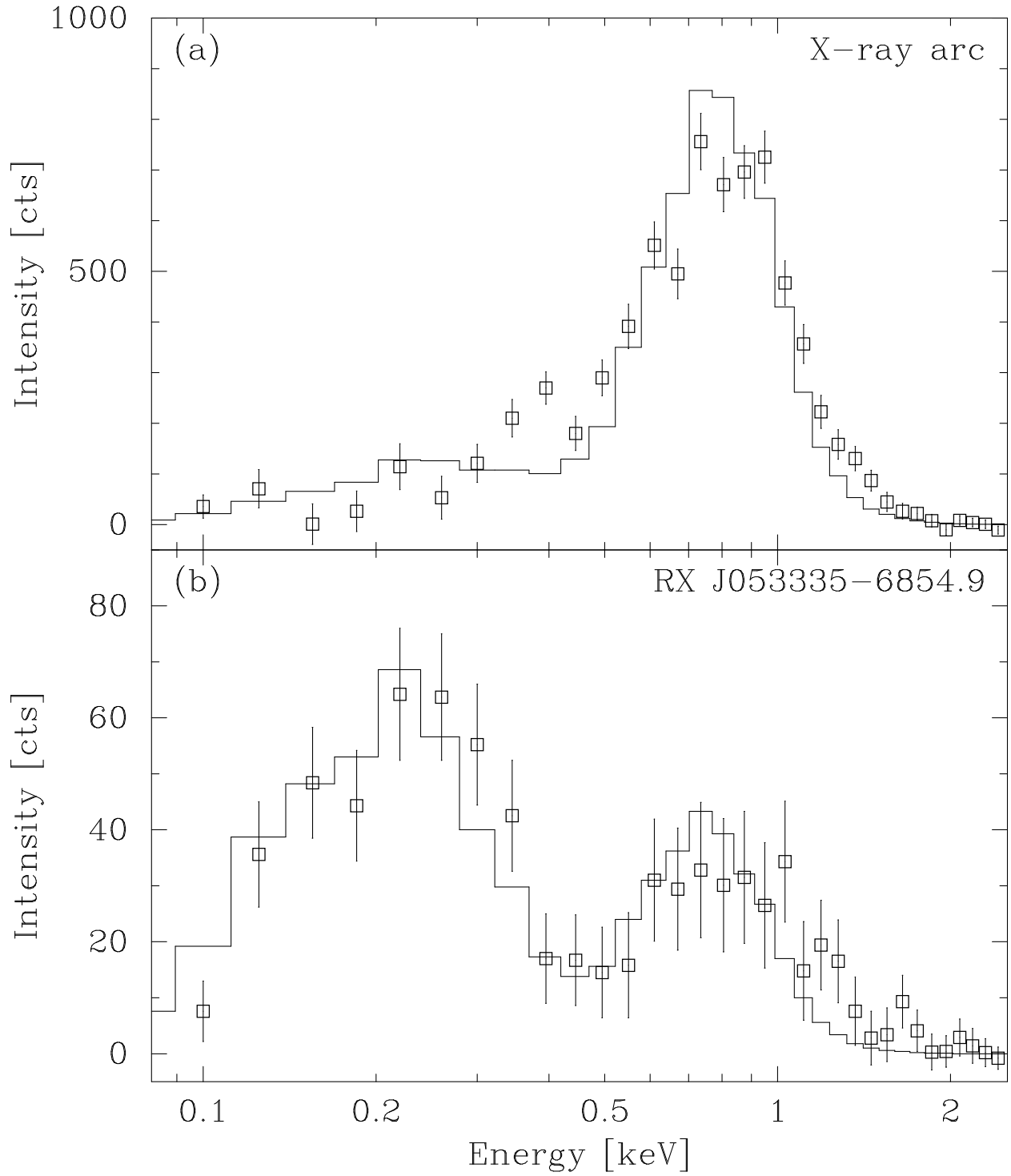


Fig. 3.— *ROSAT* PSPC spectra and best model fits of (a) the diffuse X-ray arc, and (b) the point X-ray source RX J053335-6854.9.

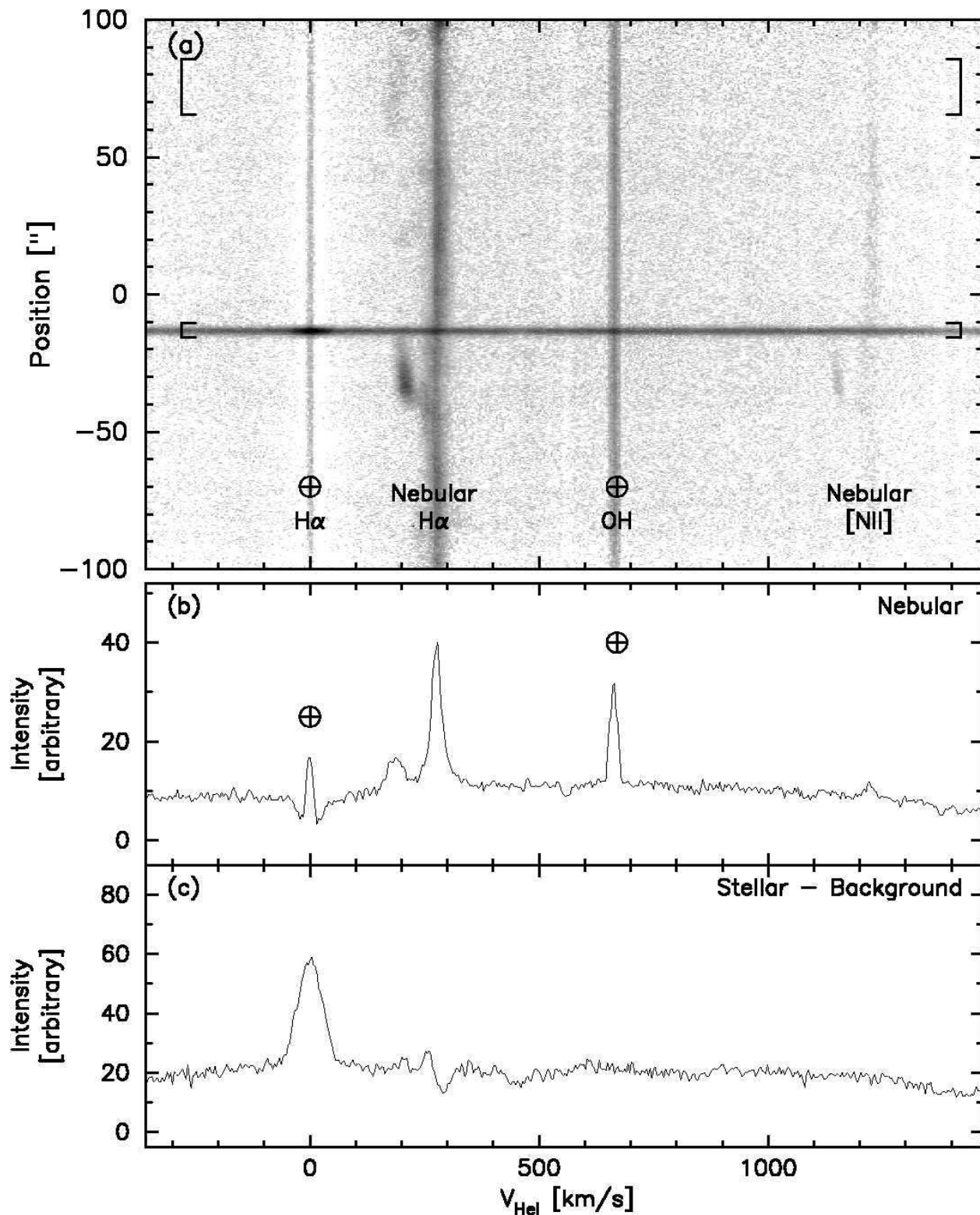


Fig. 4.— Echelle observations of the H $\alpha$ + [N II] lines: (a) the echellogram, (b) a representative H $\alpha$  line profile of the cool ionized gas, and (c) the H $\alpha$  line profile of the star. The nebular and stellar spectra were extracted from the regions marked in (a). The telluric lines are marked by “ $\oplus$ .” The observation was made during full moon, so the sky background is dominated by scattered solar radiation. The stellar spectrum in (d) is background-subtracted; the telluric lines are removed, but noticeable residuals remain in the nebular H $\alpha$  line.

Table 1. *ROSAT* Archive Observations Which Include RX J053335–6854.9

| Observation<br>Number <sup>a</sup> | Exposure<br>(s) | RA (J2000)<br>(h m s ) | Dec (J2000)<br>( ° ' " ) | Target<br>Name | Offset<br>(') |
|------------------------------------|-----------------|------------------------|--------------------------|----------------|---------------|
| RP180179N00                        | 15924           | 05 35 28.80            | –69 16 11.6              | SN1987A        | 23.5          |
| RP180251N00                        | 20153           | 05 35 28.80            | –69 16 11.6              | SN1987A        | 23.5          |
| RP180294N00                        | 2674            | 05 35 28.80            | –69 16 11.6              | SN1987A        | 23.5          |
| RP500100A00                        | 16957           | 05 35 28.80            | –69 16 11.6              | SN1987A        | 23.5          |
| RP500100A01                        | 9657            | 05 35 28.80            | –69 16 11.6              | SN1987A        | 23.5          |
| RP500140N00                        | 2642            | 05 35 28.80            | –69 16 11.6              | SN1987A        | 23.5          |
| RP500140A01                        | 11625           | 05 35 28.80            | –69 16 11.6              | SN1987A        | 23.5          |
| RP500140A02                        | 10758           | 05 35 28.80            | –69 16 11.6              | SN1987A        | 23.5          |
| RP500303N00                        | 9416            | 05 35 28.80            | –69 16 11.6              | SN1987A        | 23.5          |
| RP600100A00                        | 5803            | 05 35 38.40            | –69 16 11.6              | REGION F       | 23.9          |
| RP600100A01                        | 16865           | 05 35 38.40            | –69 16 11.6              | REGION F       | 23.9          |
| RP500131N00                        | 15959           | 05 38 33.60            | –69 06 36.0              | N157           | 29.1          |
| RP500138N00                        | 2478            | 05 26 36.00            | –68 50 23.6              | N144           | 38.2          |
| RP500138A01                        | 14531           | 05 26 36.00            | –68 50 23.6              | N144           | 38.2          |
| RP500138A02                        | 14581           | 05 26 36.00            | –68 50 23.6              | N144           | 38.2          |
| RH600640N00                        | 24070           | 05 32 04.80            | –68 51 00.0              | LMC POINT 010  | 9.1           |
| RH600634N00                        | 23619           | 05 35 52.80            | –68 51 00.0              | LMC POINT 004  | 12.9          |

<sup>a</sup>RH – HRI observations; RP – PSPC observations.